Negative Capacitance Field-Effect Transistor Based on a Two-Dimensional Ferroelectric

M. Soleimani, N. Asoudegi, P. Khakbaz, M. Pourfath*
School of Electrical and Computer Engineering
University College of Engineering
University of Tehran
Tehran, Iran
pourfath@ut.ac.ir

Abstract—Negative capacitance field effect transistors (NCFETs) based on ferroelectric materials have been the focus of intensive research activities because of their relatively small sub-threshold swing. This work proposes and presents a comprehensive study of a NCFET based on few-layer α-In_2Se_3 as the ferroelectric in order to reduce the sub-threshold swing through voltage amplification effect. By employing first principles electronic structure calculations, the Landau constants of mono and few-layer α-In_2Se_3 are extracted which were utilized for analyzing the characteristics of a NCFET with a monolayer MoS_2 as the channel material. Sub-threshold swings in the range of ∼27-59 mV/dec were achieved for few-layer α-In_2Se_3 that can be further improved by increasing the thickness of the ferroelectric layer and by using a thinner or high-κ insulate layer.

Index Terms—Negative capacitance, Transistor, Sub-threshold swing, Ferroelectric, In_2Se_3

I. Introduction

The scaling of metal-oxide-semiconductor field-effect transistors (MOS-FETs) is being limited by the inability to remove the heat generated during the switching process that originates from the poor scaling of the operating voltage (V_{DD}). A key factor that hinders the scaling of V_{DD} is the subthreshold swing (SS) which is thermally limited to ∼60 mV/dec at room temperature because of the Boltzmann statistic. The (SS)of a FET is generally given by [1]:

$$SS = \frac{\partial V_{\mathrm{G}}}{\partial(\log_{10} I_{\mathrm{D}})} = \frac{\partial V_{\mathrm{G}}}{\partial \psi_{\mathrm{S}}} \frac{\partial \psi_{\mathrm{S}}}{\partial(\log_{10} I_{\mathrm{D}})} = \left(1 + \frac{C_{\mathrm{S}}}{C_{\mathrm{Ins}}}\right)\left(\frac{\mathrm{k_B}T}{\mathrm{q}} \ln 10\right), \qquad (1)$$

where V_{G} is the gate voltage, I_{D} is the drain current, ψ_{S} is the surface potential of the semiconducting channel, C_{S} is the substrate capacitance, C_{Ins} is the gate insulator capacitance and $\mathrm{k_B}$ is the Boltzmann constant, T is the temperature, and q is the electron unit charge. At room temperature, a sub-threshold swing of approximately 60 mV/dec can be obtained if the body factor becomes close to 1. This happens if a relatively thin high-κ insulator material is used ($C_{\mathrm{S}}/C_{\mathrm{Ins}} \ll 1$). A sub-60 mV/dec for SS can be achieved if the device body factor becomes smaller than 1, where C_{Ins} can be negative while the C_{S} remains positive [2], [3]. This can be reached by using the recently proposed negative capacitance field effect transistor (NCFET), in which a ferroelectric material is added to the gate stack of conventional MOSFETs [3], [4]. Because of a negative voltage drop through the ferroelectric layer, which is due to the combination of the external electric field and polarization in the ferroelectric material, the gate voltage is amplified which in turn reduces the SS.

Two main structures are commonly studied for NCFETs: the metal-ferroelectric-metal-insulator-semiconductor (MFMIS) [5] and metal-ferroelectric-insulator-semiconductor (MFIS) [6]. It is more straightforward to realize MFMIS structures, where the inserted metal layer provides a uniform surface potential for simultaneous polarization and makes it easy to detect the internal voltage in the experiment. To obtain stabilized NC hysteretic behavior, which is the characteristic for ferroelectric materials, should be eliminated. The requirement of a hysteresis-free NC is related to the maximum critical ferroelectric thickness which can be reduced by the background permittivity.

The application of conventional ferroelectric materials for 2D channels is not optimal; therefore, this work investigates the potential of 2D ferroelectrics in NCFETs. A few 2D van der Waals (vdW) materials exhibit ferroelectricity, where for NC those with out-of-plane polarizability are of interest. An appropriate selection of a 2D ferroelectric insulator for integrating with 2D semiconductors is essential for achieving high performance NCFETs. Ferroelectric polarization switching and hysteresis loop have been recently observed down to the bilayer and monolayer (1L) α-In_2Se_3 [7] which demonstrates that the thinnest layered ferroelectrics can be realized with 2D materials.

This work proposes and presents a comprehensive study on a NCFET based on the MFMIS structure, where a monolayer MoS_2 serves as the channel material and few-layer α-In_2Se_3 acts as the ferroelectric material. As shown in Fig.1(a), compared to the conventional MOSFETs, the NCFETs have an additional ferroelectric layer deposited on the metal gate. Recent experiments indicate that in the

978-1-7281-0940-4/19/$31.00 ©2019 IEEE

employed structure the metal gate provides the same gate charge density to both the internal gate and ferroelectric surfaces [5], [8]. The NCFETs can be described by the capacitor divider model of Fig.1(b), where C_{Fe}, C_{Ins} and C_{S} are the capacitors due to the ferroelectric layer, the dielectric layer and the semiconductor, respectively. The total gate capacitance of a NCFET (C_{G}) consists of a series combination of C_{Ins} and C_{Fe}.

In this paper, we focus on the α-In_2Se_3 as the ferroelectric material shown in Fig.1(c). First principle calculations based on density functional theory (DFT) are applied to systematically study the electronic properties of α-In_2Se_3 through layer-dependent cleavage energy, Gibbs free energy, polarization, averaged electrostatic potential energy and bandgap. Using the electronic structure calculations we determine the Landau constants of α-In_2Se_3 and quantitatively investigate the device properties of the NCFET.

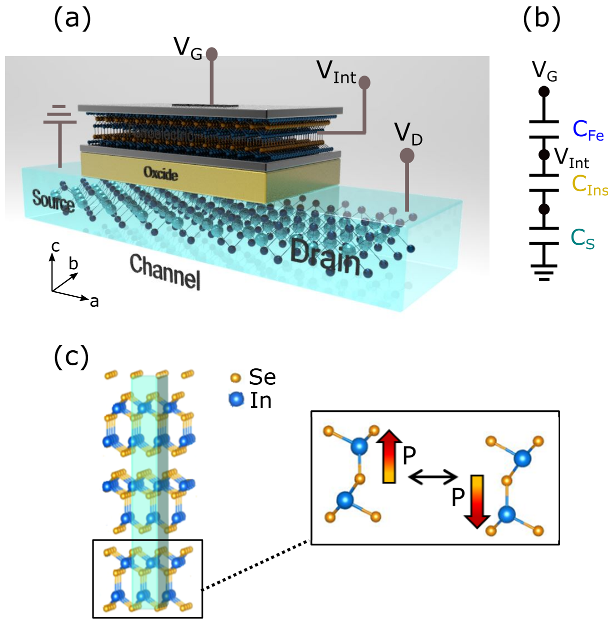

Fig. 1: The schematic of a NCFET with monolayer MoS_2 as the channel material and α-In_2Se_3 as the ferroelectric. (b) The equivalent capacitor model for the combination of the gate, ferroelectric and insulator in the MFMIS structure. (c) The atomistic structure of layered α-In_2Se_3 ferroelectric. α-In_2Se_3 switching from the upward polarization (top) to the downward polarization (bottom).

II. Approach

To model the current-voltage characteristic of nanoscale transistors, the top-of-the barrier model proposed in Ref. [9] has been utilized. The drain-source current can be obtained by:

$$I_{\text{DS}} = \int_{-\infty}^{+\infty} J\left(E - U_{\text{scf}}\right)\left[f_1\left(E\right) - f_2\left(E\right)\right] dE, \qquad (2)$$

where f_1, f_2 are the Fermi-Dirac distribution functions of the contacts and J is the current density, and U_{scf} is the self-consistent potential at the top of the barrier along the channel. To model the dynamics of ferroelectric polarization, the Landau-Khalatnikov (LK) equation can be used [3]:

$$\rho \frac{d\vec{P}}{dt} + \nabla_{\vec{P}} G = 0, \qquad (3)$$

where ρ and P are the resistivity and polarization, respectively. Here, F represents the Gibbs free energy of the ferroelectric material and is a function of a series expansion of the polarization as:

$$F = aP^2 + bP^4 + cP^6 - \vec{E}_{\text{ext}}.\vec{P}, \qquad (4)$$

where a, b and c are Landau coefficients and $\vec{E}_{\text{ext}}$ is the external electric field. The gate voltage of the NCFET can be written as

$$V_{\text{G}} = V_{\text{Int}} + \left[2aQ_{\text{G}} + 4bQ_{\text{G}}^3\right] t_{\text{Fe}}, \qquad (5)$$

where V_{Int} is the internal voltage the second term is the voltage drop across the ferroelectric. Also, t_{Fe} and Q_{G} are the ferroelectric thickness and gate charge density, respectively.

DFT calculations have been carried out within the framework of the projector augmented-wave (PAW) formalism [10], [11] as implemented in the Vienna Ab initio Simulation Package (VASP). Structural relaxations and calculation of the electronic properties were carried using the generalized gradient approximation (GGA) as parameterized by Perdew-Burke-Ernzerhof functional for solids (PBEsol) [12] with a convergence criterion that forces on the atoms become smaller than 0.001 eV/Å. For the bandgap calculations, we also used the hybrid functional of Hyed-Scuseria-Ernzerhof (HSE06) [13] The plane wave cutoff energy is 500 eV and a 12×12×1 grid points were used in k-space to sample the Brillouin zone. The dispersion interaction was accounted for layered α-In_2Se_3 by using the Grimme's DFT-D3 method [14]. The Gibbs free energy under mild conditions of temperature, T=300 K can be expressed as

$$F = H^0 + TS + \text{ZPE}, \qquad (6)$$

where H^0, S and ZPE are the enthalpy at absolute zero, the entropy and intrinsic zero point energy.

III. Results and Discussion

Cleavage energies of α-In_2Se_3 1L and 2L from a five-layer (5L) slab were calculated to confirm feasibility of getting a 1L and 2L α-In_2Se_3 by exfoliation. As shown in Fig.2(a), the cleavage energies required to slice the 1Land 2L α-In_2Se_3 along c plane are 0.60 J/m^2 and 0.66 J/m^2, respectively. It should be noted that the cleavage energy of slicing bulk α-In_2Se_3 into 1L and 2L is close to that of slicing graphite into graphene (0.36 J/m^2) [15]. This indicates that slicing the α-In_2Se_3 into 2D monolayers along a specific plane is highly feasible.

Fig.2(b) shows the Gibbs free energy for 1L to 5L α-In_2Se_3 at room temperature. It is found that, thicker α-

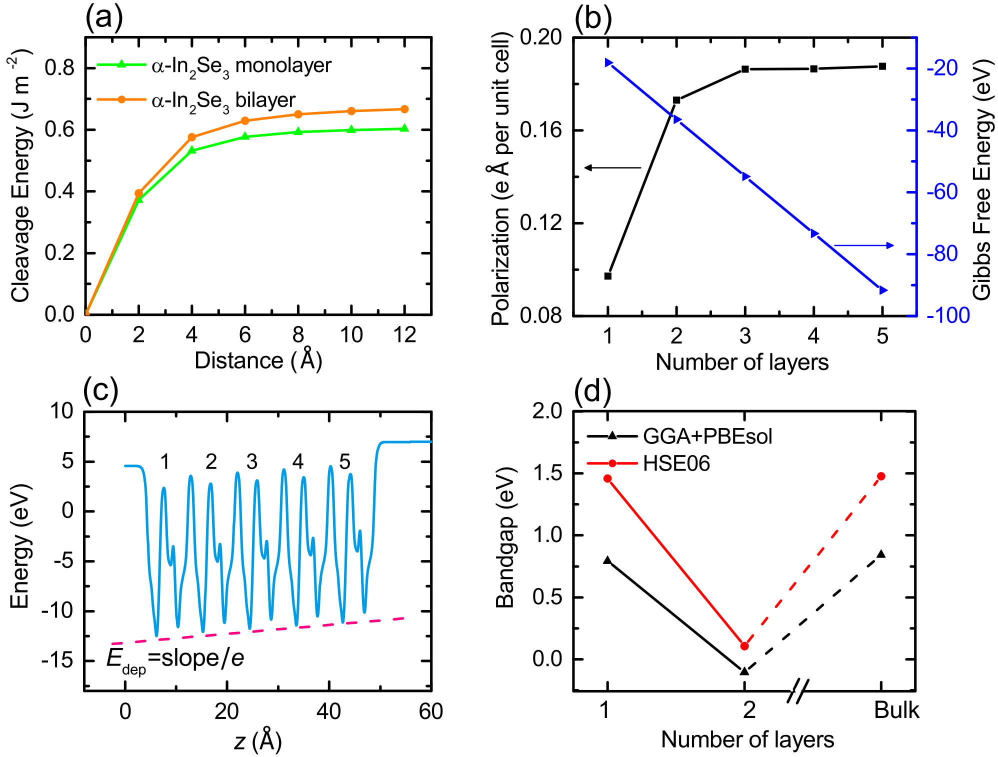

Fig. 2: The cleavage energies estimation regarding the slicing of α-In_2Se_3 along c plane the structure of α-In_2Se_3, (b) the polarization and Gibbs free energies at T=300 K, (c) the planar-averaged electrostatic potential energy along c plane for 5L α-In_2Se_3. (d) Evolution of bandgap as a function of the number of layers with the GGA-PBEsol and HSE06 methods, respectively.

In_2Se_3 is more stable than monolayer of this materials. The difference in stability between monolayer and few-layer α-In_2Se_3 is related to the vdW coupling between the α-In_2Se_3 layers. In addition, Fig.2(b) indicates that the average out-of-plane polarization of the 2L is over two times larger than that of the monolayer and the magnitude of the electric dipole saturates beyond two layers. The absence of the energy band gap and overlaying of the conduction and valence bands above 2L lead to charge transfer induced by the depolarization field on both surfaces of the film which in turn hinders further increase of the polarization.

The average electrostatic potential energy in the c plane for 5L α-In_2Se_3 is shown in Fig.2(c). Also, the depolarization field E_{dep} was calculated from the electrostatic potential energy. The depolarization fields of the 5L are not completely compensated, and the values decrease as the number of layers increases and will disappear in thick films. Fig.2(d) indicates the bandgap evolution as a function of the number of layers. Due to the existence of bandgap underestimation in GGA-PBEsol functional, we also employed the hybrid functional approximation using HSE06 exchange-correlation term. It was obvious that there was a bandgap shortening from the monolayer to bilayer by both methods. Bandgaps of α-In_2Se_3 are extracted as 1.46 eV (1L), 0.11 eV (2L) and 1.48 eV (bulk).

To analyze α-In_2Se_3 as the ferroelectric in NCFET, the Landau constants are extracted (Table.I) from the Gibbs free energy at T=300 K versus polarization during the phase transition.

TABLE I: Landau constants extracted by fitting parameters in Eq. (4).

α-In_2Se_3	a (V/eÅ^2)	b (V/e^{3}Å^4)
1L	-28.65	14.575e+2
2L	-6.96	116.27
Bulk	-2.75	48.40

In an NCFET, the external gate voltage V_{G} induces polarization within the ferroelectric. The net charge density inside the ferroelectric capacitor, defined as the difference between the polarization-induced surface charge and the screening charge density, determines the voltage drop across a ferroelectric V_{Fe}. The negative capacitance appears appears when the polarized charges are not completely screened during the switching of polarization [4]. This implies that the voltage drop across the ferroelectric is a negative quantity and $V_{\mathrm{FET}} > V_{\mathrm{G}}$ (from$V_{\mathrm{G}} = V_{\mathrm{FET}} + V_{\mathrm{Fe}}$), where V_{FET} is the voltage across the MOS-FET. Therefore, the same charge density can be achieved in the channel with a smaller gate voltage which leads to a SS steeper than 60 mV/dec [16].

As shown in Fig.3(a) SS=67 mV/dec for MoS_2-FET, while the NCFET with a 5 nm (5L) α-In_2Se_3 achieved the SS of 59 mV/dec that is reduced to 27 mV/dec for 25

nm. By increasing the thickness of the ferroelectric layer, the performance enhancement increases because of the reduction of C_{Fe}, ($| C_{Fe} | \sim C_{FET}$), which in turn results in larger amplification of the gate voltage. In addition a more direct way to improve the device performance is the increasing the capacitance of the insulator layer. The dependence of the C_{Ins} on the EOT suggests that thinner gate insulators result in smaller SS Also, the SS of NCFET can be further improved by using high-κ insulate layer. In Fig.3(b) different EOT and gate insulator layer materials are applied in the NCFET with a 5 nm ferroelectric layer. It can be seen that the SS can reach smaller than 60 mV/dec by using thinner or high-κ insulate layer.

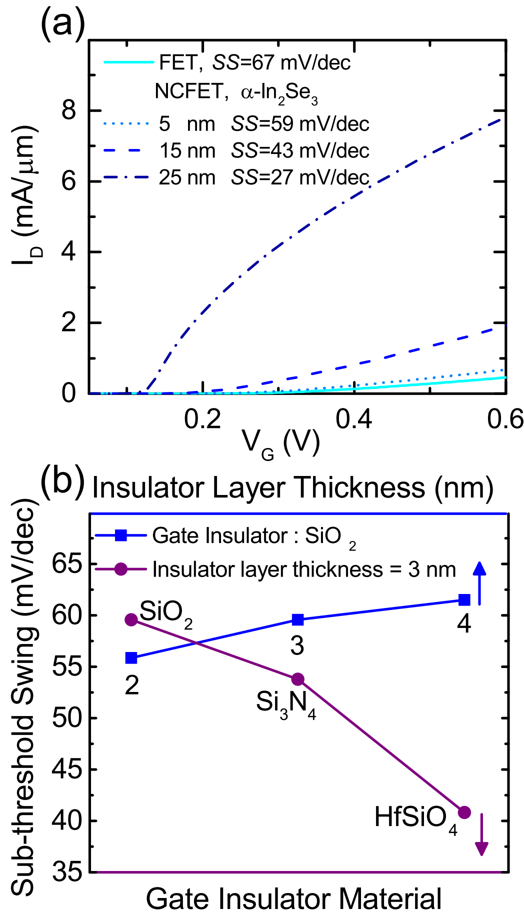

Fig. 3: (a) I_D-V_G for a MoS_2-based FET and NCFETs at V_D=0.6 V with a 3 nm SiO_2 insulator layer for various thicknesses of α-In_2Se_3. (b) The SS at various thicknesses of insulator layer and gate insulator materials for NCFET with 5 nm α-In_2Se_3.

IV. Conclusion

This work presents a comprehensive study of NCFETs with monolayer MoS_2 as the channel material and few-layer α-In_2Se_3 as the ferroelectric material. First principles calculations were employed for determining the electronic properties and extracting Landau constants of the α-In_2Se_3. Monolayer α-In_2Se_3 as the thinnest layered ferroelectric reveals the out-of-plane polarization. The SS in the range of ~27-59 mV/dec were achieved for 25 nm to 5 nm of α-In_2Se_3 which can be further reduced by using thicker α-In_2Se_3 and thinner or high-κ insulate layer. The presented results pave the way for realizing high performance 2D NCFETs.

Acknowledgements

This work was partly supported by Iran National Science Foundation (INSF).

References

[1] R. J. Van Overstraeten, G. J. Declerck, and P. A. Muls, "Theory of the mos transistor in weak inversion-new method to determine the number of surface states," IEEE T-ED, vol. 22, pp. 282–288, May 1975.
[2] A. M. Ionescu and H. Riel, "Tunnel field-effect transistors as energy-efficient electronic switches," nature, vol. 479, p. 329, November 2011.
[3] S. Salahuddin and S. Datta, "Use of negative capacitance to provide voltage amplification for low power nanoscale devices," Nano lett., vol. 8, pp. 405–410, March 2008.
[4] V. V. Zhirnov and R. K. Cavin, "Nanoelectronics: Negative capacitance to the rescue?" Nat. Nanotechnol., vol. 3, p. 77, February 2008.
[5] J. Jo, W. Y. Choi, J.-D. Park, J. W. Shim, H.-Y. Yu, and C. Shin, "Negative capacitance in organic/ferroelectric capacitor to implement steep switching mos devices," Nano lett., vol. 15, pp. 4553–4556, June 2015.
[6] X. Wang, Y. Chen, G. Wu, D. Li, L. Tu, S. Sun, H. Shen, T. Lin, Y. Xiao, M. Tang et al., "Two-dimensional negative capacitance transistor with polyvinylidene fluoride-based ferroelectric polymer gating," NPJ 2D Mater. Appl., vol. 1, p. 38, November 2017.
[7] F. Xue, W. Hu, K.-C. Lee, L.-S. Lu, J. Zhang, H.-L. Tang, A. Han, W.-T. Hsu, S. Tu, W.-H. Chang et al., "Room-temperature ferroelectricity in hexagonally layered α-in2se3 nanoflakes down to the monolayer limit," Adv. Funct. Mater., vol. 28, p. 1803738, October 2018.
[8] G. Pahwa, T. Dutta, A. Agarwal, and Y. S. Chauhan, "Physical insights on negative capacitance transistors in nonhysteresis and hysteresis regimes: Mfmis versus mfis structures," IEEE T-ED, vol. 65, pp. 867–873, January 2018.
[9] A. Rahman, J. Guo, S. Datta, and M. S. Lundstrom, "Theory of ballistic nanotransistors," IEEE T-ED, vol. 50, pp. 1853–1864, September 2003.
[10] P. E. Blöchl, "Projector augmented-wave method," Phys. Rev. B, vol. 50, p. 17953, December 1994.
[11] G. Kresse and D. Joubert, "From ultrasoft pseudopotentials to the projector augmented-wave method," Phys. Rev. B, vol. 59, p. 1758, January 1999.
[12] J. P. Perdew, A. Ruzsinszky, G. I. Csonka, O. A. Vydrov, G. E. Scuseria, L. A. Constantin, X. Zhou, and K. Burke, "Restoring the density-gradient expansion for exchange in solids and surfaces," Phys. Rev. Lett., vol. 100, p. 136406, April 2008.
[13] J. Heyd, J. E. Peralta, G. E. Scuseria, and R. L. Martin, "Energy band gaps and lattice parameters evaluated with the heyd-scuseria-ernzerhof screened hybrid functional," J. Chem. Phys., vol. 123, p. 174101, October 2005.
[14] S. Grimme, J. Antony, S. Ehrlich, and H. Krieg, "A consistent and accurate ab initio parametrization of density functional dispersion correction (dft-d) for the 94 elements h-pu," J. Chem. Phys., vol. 132, p. 154104, March 2010.
[15] R. Zacharia, H. Ulbricht, and T. Hertel, "Interlayer cohesive energy of graphite from thermal desorption of polyaromatic hydrocarbons," Phys. Rev. B, vol. 69, p. 155406, April 2004.
[16] K. Ng, S. J. Hillenius, and A. Gruverman, "Transient nature of negative capacitance in ferroelectric field-effect transistors," Solid State Commun., vol. 265, pp. 12–14, October 2017.